Beam profile monitor data analysis

Ping Zhou

October 14, 1994

1 Introduction

In the AGS to RHIC transfer line beam profile monitors employing phosphor screens will be used to measure two dimensional beam profile and derive the beam emittance and Twiss parameters. This note present the details as well as summarizes the planned analysis.

There will be eight profile monitors, also called flags, installed in the injection line, the transfer line less the two arcs at the end, test. Four of them can be used for simultaneous operation because of the total number of video frame grabbers available.

2 Limitations and Assumptions

In addition to the horizontal and vertical beam density distribution, the two dimensional beam profiles contain information on beam coupling in the two directions. This information can be used to identify and in feedback to correct the possible coupling of beams coming out of AGS. If significant coupling is present a complete four dimensional phase space analysis, ignoring the even more complicated additional coupling with the longitudinal dimension, is necessary. A meaningful and reliable complete phase space analysis is impossible by virtue of the number of flags, the necessary measurement accuracy and the complexity of the required analysis. We will limit ourselves to the analysis of one dimension at a time and assume the coupling effect to be negligible after correction. Under these assumptions we need only one di-

mensional beam profiles, which can be obtained by projecting the 2-D profile onto the horizontal and vertical directions.

In some parts of the analysis we will also assume the beam has a phase space density distribution with elliptical symmetry. This has been one of the basis for most modern accelerator beam analysis and will be implied throughout the note unless stated otherwise.

3 Beam widths and the measurement errors

As we will see later in this note, emittance and Twiss parameters calculation is based on three or more beam widths, at different locations or the same location with different lattices. The errors in the beam profile measurement and thereof calculated beam width directly leads to errors in the calculation of beam emittance and Twiss parameters. We will start by estimating the errors in the beam widths resulting from the profile noises.

The measured beam profile and the symbols used hereafter are illustrated in Figure 1.

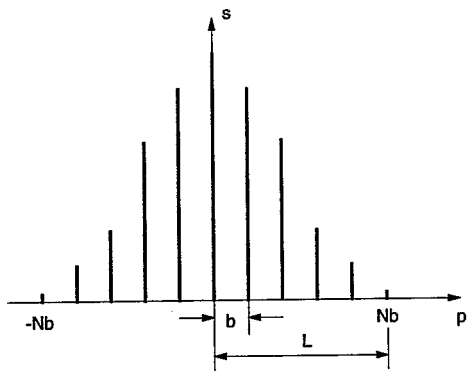

Figure 1: An illustration of symbols.

The random measurement error in s_i consists of two parts, the statistical part and the external noise part. Since the interaction between beam particles and the phosphor screen material is of random nature, the statistical fluctuation of the signal will always exist. The signal is proportional to the number of particles, i.e. $s_i = kN$ where N is the total number of particles

Flag Name	σ (mm)		Resolution (mm)	
	Horizontal	Vertical	Horizontal	Vertical
UF1	2.9	0.7	0.21	0.14
UF2	0.9	0.9	0.12	0.10
UF3	1.3	2.9	0.19	0.16
UF4	2.7	1.3	0.15	0.13
UF5	1.3	2.7	0.17	0.15
WF1	3.0	0.9	0.16	0.13
WF2	0.9	3.6	0.19	0.16
WF3	3.7	1.1	0.19	0.16

Table 1: Overall resolutions for flags in U and W-lines.

covered by the one data point and k is the overall gain of the system. The statistical fluctuation in the signal is thus $k\sqrt{N}$ and the ratio to the signal is $1/\sqrt{N}$. Since the number of particles involved is usually very large in our application, and keep in mind that our system has a maximum signal resolution of 255:1 (8 bit), I have neglected the error introduced by the random fluctuation. The rest of the error, introduced by e.g. electronic noise, is assumed to be independent at each data point and have the same amplitude for all data points, i.e.

$$\Delta s_i = \Delta s \tag{1}$$

There is also systematic error associated with each measurement, resulting from the limited resolution of the optical system. Lens aberration, depth-of-field and CCD resolution all contribute to this limitation. The effect on the measurement would be the broadening of the image and hence the beam profile. The observed profile is the convolution of the real beam profile and the broadening distribution and the square of the measured rms beam width is the sum of the square of the real rms beam width and the square of the rms broadening. The effect can be estimated from the optical calculation and camera resolution measurement. This has been done[1] and the overall resolution for all the transfer line flags are listed in Table 1. For most part this effect only result in a small increase in the measured beam width, therefore we will treat this as a measurement error rather than trying to extract the undistorted beam width.

The width parameter can be obtained through either direct calculation

or after fitting the profile to a known functional form. They have different implications in terms of handling measurement errors. Given the assumption about measurement error, the points far from beam center have little to contribute to the profile signal, but equal contribution in the error compared to the central data points. Function fitting has the advantage of less susceptible to the noise far from the beam center and contains more shape information, but involves choosing the appropriate function or function set in anticipating of the beam profile form and probably much more intensive calculation. For our purpose here we will only deal with rms beam width and hence rms beam emittance. We will therefore only deal with direct calculation here and leave the fitting approach for future consideration if there is sufficient need for the distribution shape information.

Suppose the measured 1-D beam profile is S_i and the position of the i-th point is x_i, we then have

$$\begin{aligned} \overline{x} &= \sum_i x_i s_i / \sum_i s_i \\ \overline{x^2} &= \sum_i x_i^2 s_i / \sum_i s_i \end{aligned} \tag{2}$$

The rms beam width w is given by

$$w^2 = \overline{x^2} - \overline{x}^2 \tag{3}$$

The window size must be big enough to cover most of the beam, but since the tail contains little beam and yet contributes noise equally to the result as central data points, the window should not be unnecessarily big. A reasonable size window would be about two times the rms beam width centered around the beam center. For a beam with Gaussian profile, this would enclose 95% of the beam.

3.1 Error bounds

The total signal, which is proportional to the total beam charge, and its fluctuation amplitude are

$$\begin{aligned} Q &= \sum_i s_i \\ \Delta Q &= (\sum_i 1)\Delta s = \frac{2L}{b}\Delta s \end{aligned} \tag{4}$$

The rms beam width and its error bounds are

$$w^2 = \overline{x^2} - \overline{x}^2 = \frac{1}{Q}\sum_i x_i^2 s_i - \frac{1}{Q^2}(\sum_i x_i s_i)^2 \tag{5}$$

$$\begin{aligned} \Delta w^2 &= \sum_i \left|\frac{\partial w^2}{\partial s_i}\right| \Delta s_i \\ &= \sum_i \frac{1}{Q}\left|x_i^2 - \overline{x^2} - 2\overline{x}(x_i - \overline{x})\right| \Delta s \end{aligned} \tag{6}$$

Since $N \gg 1$ we can use integration to estimate Eq. 6. Put in the case where the beam is about centered in the window, i.e. $\overline{x} \approx 0$, and $L/w \approx 2$, we have

$$\begin{aligned} \Delta w^2 &\approx \frac{\Delta s}{Q}\int_{-L}^{L}\left|x^2 - \overline{x^2} - 2\overline{x}(x - \overline{x})\right| \frac{dx}{b} \\ &= \frac{2\Delta s}{Q}\left[\int_0^w (w^2 - x^2)\,dx + \int_w^L (x^2 - w^2)\,dx\right] \\ &= \frac{L^3 \Delta s}{2bQ} \\ &= \frac{L^2}{4}\frac{\Delta Q}{Q} \end{aligned} \tag{7}$$

which is simply

$$\frac{\Delta w^2}{w^2} \approx \frac{1}{2}\frac{\Delta Q}{Q} \tag{8}$$

3.2 rms error

Since the error in beam rms width is assumed to be caused by the independent error source at each data point, we can also estimate the rms error in w^2 as:

$$\sigma_{w^2}^2 = \sum_i (\frac{\partial w^2}{\partial s_i})^2 \cdot \sigma_n^2 \tag{9}$$

where σ_n is the rms error at each profile data point. Using Eq. 3 we have

$$\begin{aligned} \frac{\partial w^2}{\partial s_i} &= \frac{1}{Q}x_i^2 - \frac{2}{Q}x_i \sum_j x_j s_j - \left[\frac{1}{Q^2}\sum_i x_i^2 s_i - \frac{2}{Q^3}(\sum_i x_i s_i)^2\right] \cdot \frac{\partial Q}{\partial s_i} \\ &= \frac{1}{Q}\left[x_i^2 - 2x_i\overline{x} - (\overline{x^2} - 2\overline{x}^2)\right] \\ &= \frac{1}{Q}\left[(x_i - \overline{x})^2 - w^2\right] \end{aligned} \tag{10}$$

and

$$\sum_i (\frac{\partial w^2}{\partial s_i})^2 = \sum_i \frac{1}{Q^2}\left[(x_i - \overline{x})^2 - w^2\right]^2 \tag{11}$$

Again, we can use the integration to estimate Eq. 11:

$$\begin{aligned} &\sum_i \left[(x_i - \overline{x})^2 - w^2\right]^2 \\ &\approx \frac{1}{b}\int_{-L}^{L}\left[(x - \overline{x})^2 - w^2\right]^2 dx \\ &= \frac{L^5}{b}\left\{\frac{1}{5}\left[(1 - \frac{\overline{x}}{L})^5 + (1 + \frac{\overline{x}}{L})^5\right]\right. \\ &\quad \left. -\frac{2}{3}\frac{w^2}{L^2}\left[(1 - \frac{\overline{x}}{L})^3 + (1 + \frac{\overline{x}}{L})^3\right] + 2(\frac{w}{L})^4\right\} \end{aligned} \tag{12}$$

For the case of $\overline{x}/L \approx 0$ and $L/w \approx 2$ we have

$$\sum_i \left[(x_i - \overline{x})^2 - w^2\right]^2 \approx 0.2\frac{L^5}{b} \approx 1.6\, w^2 \frac{2L}{b} \tag{13}$$

Since

$$\sigma_Q^2 = \sum_i \sigma_n^2 \approx \frac{2L}{b}\sigma_n^2 \tag{14}$$

Equation 9 leads to

$$\frac{\sigma_{w^2}}{w^2} \approx \frac{\sigma_Q}{Q} \tag{15}$$

4 Twiss parameters and emittance calculation

Among the four quantities we are interested, α, β, γ and ϵ, only three are independent. Determining them requires three or more beam width measurements. The number of measurements does not necessarily mean the number of flags in simultaneous measurement. It could be total number of flags at different locations with multiple beam bunches, assuming a very good repeatability from bunch to bunch. It could also be the number of measurements with one or more flags at the same place but with varying magnet settings. Again bunch to bunch jitter has to be negligible for the calculation to be meaningful. With more than three measurements some kind of fitting has to be used to determine the best value for the parameters. We will use the least square fit here.

We will summarize the calculation of beam emittance and Twiss parameters from beam width measurements here. Details can be found in [2][3] and [4].

Suppose we want to solve for the parameters at location s_0 and we make the three quantities be

$$\begin{aligned} a_1 &= \epsilon\beta \\ a_2 &= \epsilon\alpha \\ a_3 &= \epsilon\gamma \end{aligned} \tag{16}$$

With the lattice transfer matrix from s_0 to s_i being

$$T = \begin{pmatrix} t_{11} & t_{12} \\ t_{21} & t_{22} \end{pmatrix} \tag{17}$$

Twiss parameters at s_i are[5]

$$\begin{pmatrix} \beta \\ \alpha \\ \gamma \end{pmatrix}_i = \begin{pmatrix} t_{11}^2 & -2t_{11}t_{12} & t_{12}^2 \\ -t_{11}t_{21} & 1+2t_{12}t_{21} & -t_{12}t_{22} \\ t_{21}^2 & -2t_{21}t_{22} & t_{22}^2 \end{pmatrix} \begin{pmatrix} \beta \\ \alpha \\ \gamma \end{pmatrix}_0 \tag{18}$$

The beam width measured with i-th flag at s_i can thus be written as

$$y_i \equiv w_i^2 = \beta_i \epsilon = \sum_k g_{ik} \cdot a_k \tag{19}$$

where

$$\begin{aligned} g_{i1} &= t_{11}^2 && (20)\\ g_{i2} &= -2t_{11} \cdot t_{12} && (21)\\ g_{i3} &= t_{12}^2 && (22) \end{aligned}$$

Notice that g_{ik} only involves the elements fro the first row of the matrix in Eq. 17.

Minimizing

$$\chi^2 = \sum_i \left[\frac{y_i - \sum_k g_{ik} \cdot a_k}{\sigma_i} \right]^2, \tag{23}$$

where σ_i is the rms error in w_i^2, yields the normal equation for the problem

$$[N_{jk}]\,(a_k) = (b_j) \tag{24}$$

where

$$\begin{aligned} N_{jk} &= \sum_i \frac{g_{ij} \cdot g_{ik}}{\sigma_i^2} && (25)\\ b_j &= \sum_i \frac{g_{ij} \cdot y_i}{\sigma_i^2} && (26) \end{aligned}$$

Let $[V] = [N]^{-1}$ the solution to Eq. 24 is simply

$$(a_j) = [V_{jk}]\,(b_k) \tag{27}$$

and the standard errors in a_j are also contained in the matrix $[V]$:

$$\sigma_{a_j}^2 = V_{jj} \tag{28}$$

In fact the standard error for any other dependent variable, $f = f(a_i)$, can be easily calculated with $[V]$:

$$\sigma_f^2 = \sum_i \left(\frac{\partial f}{\partial y_i} \right)^2 \sigma_i^2 = \sum_{m,n} \frac{\partial f}{\partial a_m} \cdot V_{mn} \cdot \frac{\partial f}{\partial a_n} \tag{29}$$

f	$\frac{\partial f}{\partial a_1}$	$\frac{\partial f}{\partial a_2}$	$\frac{\partial f}{\partial a_3}$
ϵ	$\frac{1-\alpha^2}{2\epsilon}$	$\frac{\alpha\beta}{\epsilon}$	$-\frac{\beta^2}{2\epsilon}$
β	$-\frac{\alpha\gamma}{2\epsilon}$	$\frac{\beta\gamma}{\epsilon}$	$-\frac{\alpha\beta}{2\epsilon}$
α	$-\frac{\gamma^2}{2\epsilon}$	$\frac{\alpha\gamma}{\epsilon}$	$-\frac{\alpha\beta}{2\epsilon}$
γ	$-\frac{\gamma^2}{2\epsilon}$	$\frac{\alpha\gamma}{\epsilon}$	$\frac{1-\alpha^2}{2\epsilon}$

Table 2: Partial derivatives

The beam emittance and Twiss parameters at s_0 are then

$$\begin{aligned} \epsilon &= \sqrt{a_1 \cdot a_3 - a_2^2} \\ \beta &= \frac{a_1}{\epsilon} \\ \alpha &= \frac{a_2}{\epsilon} \\ \gamma &= \frac{a_3}{\epsilon} \end{aligned} \tag{30}$$

with the partial derivatives given in Table 2. Standard errors for Twiss parameters at any other location can be easily obtained using Eqs. 18 and 29 and Table 2.

The three flag calculations done with simulation show that with 10% rms error in the measured beam widths, the standard error in calculated beam emittance varies from a few percent to above 20% depending on which three flags are used. Using more flags reduces this error with the magnitude of the reduction depending also on the flag. This fluctuation of errors is mainly determined by the inter-flag betatron phase advances and usually refects the goodness of the flag location selections.

The parameters in Eq. 17 can be expressed as funtions of the phase advance between the two points:

$$t_{11} = \sqrt{\frac{\beta_i}{\beta_0}}(\cos\Delta\psi + \alpha_i \sin\Delta\psi) \tag{31}$$

$$t_{12} = \sqrt{\beta_0\beta_i}\,\sin\Delta\psi \tag{32}$$

$$t_{21} = -\frac{(1+\alpha_0\alpha_i)\sin\Delta\psi + (\alpha_i - \alpha_0)\cos\Delta\psi}{\sqrt{\beta_0\beta_i}} \tag{33}$$

$$t_{22} = \sqrt{\frac{\beta_0}{\beta_i}}(\cos\Delta\psi - \alpha_i \sin\Delta\psi) \tag{34}$$

Suppose the two flags are located at location $s = s_0$ and $s = s_i$, then when $\Delta\psi = n\pi$, $t_{12} = 0$ and $g_{i2} = g_{i3} = 0$. It follows that the $[N_{jk}]$ matrix in Eq. 25 will be singular which simply When the phase advance is close but equal to multiples of 180 degrees, theoretically the problem is perfectly solvable, but the result is increasingly sensitive to small errors in beam width measurements. However, we have to point out that the phase advance is highly dependent on initial beam parameters as well as the transfer line lattice, so what actually turn out in actual measurements may be different from bunch to bunch.

5 Phase space distribution reconstruction

The beam phase space distribution can be reconstructed from the density profiles measured with the flags, provided the distribution has elliptical symmetry. Having the full 2-dimensional phase space distribution makes the calculation of partial beam emittance easy and convenient. There have been percentage emittance calculations reported with various assumption[3][2]. Elliptical symmetry is the least assumptions needed for this purpose.

A 2-dimensional beam phase space distribution with elliptical symmetry, $\rho(x, x') = \rho(\gamma x^2 + 2\alpha x x' + \beta x'^2)$, can be transformed into a circular distribution in (u, v) space with the transformation

$$\begin{pmatrix} u \\ v \end{pmatrix} = \frac{1}{\sqrt{\beta}} \begin{pmatrix} 1 & 0 \\ \alpha & \beta \end{pmatrix} \begin{pmatrix} x \\ x' \end{pmatrix} \tag{35}$$

The resulting distribution will be $\rho(u^2+v^2)$. The projection of the phase space distribution which is the 1-dimensional beam profile that can be measured with a flag is

$$\int \rho(x,x')\,dx' = \frac{1}{\sqrt{\beta}}\int \rho(u,v)\,dv \tag{36}$$

Since $\rho(u,v)$ has circular symmetry, i.e. $\rho(u,v)=\rho(u^2+v^2)$, the distribution can be recovered from the projection through inverse Abel transform[6]. Once we get the phase space distribution through the Abel inversion, beam profile and hence the corresponding emittance for any fraction of the total beam can be calculated.

5.1 Abel transformation and the inversion

For a function with circular symmetry in (x,y) space, $f(x,y)=f(r)$, its Abel transform is simply the projection onto one of its axis:

$$f_A(x) = \int_{-\infty}^{\infty} f(r)\,dy = 2\int_x^{\infty} \frac{f(r)r\,dr}{\sqrt{r^2-x^2}} \tag{37}$$

The inversion is

$$f(r) = -\frac{1}{\pi}\int_r^{\infty} \frac{f_A'(x)\,dx}{\sqrt{x^2-r^2}} \tag{38}$$

The direct inversion in Eq. 38 involves derivation and divergent function and therefore is not suited for numerical applications. There are various ways to get around the problem[7], including the filtering of raw data to reduce noise, using transform techniques to avoid the divergence. One can also fit the data to analytical functions based on physical models and carry out the inversion analytically. In our case we will implement the latter approach now, and other techniques later if the current one is found inappropriate or inefficient based on numerical or real experiments.

We choose Gaussian weighted Hermite polynomials to expand the beam profile:

$$\rho(x) = \sum_n h_n\, H_n(\frac{x}{\sigma})\, e^{-\frac{1}{2}(\frac{x}{\sigma})^2} \tag{39}$$

Because this set of functions are orthogonal, we can avoid the fitting of parameters thus simplifying the calculation of expansion coefficients. Since the

undistorted profile should be symmetric about the center, based on the elliptical phase space distribution assumption, we only need the even orders of Hermite polynomials. The maximum order that has to be used in the expansion, however, is not as small as we might have expected or hoped, even when the profile is close to a Gaussian distribution. This is because errors in the calculation of rms of the profile will introduce many high order components. As a result 10 to 20 terms have to be included usually. Thankfully, the expansion process itself is very fast and high number of terms does not constitute much inefficiency in the overall reconstruction process.

The Abel inversion of the Gaussian weighted Hermite polynomials can be calculated analytically. The values of the functions, their Abel inversions and the fraction inside any radius can all be calculated through recursion relationsA. The result of the inversion can be summarized as

$$\rho(r) = \sum_n a_n \, r^n \, e^{-\frac{r^2}{2}}. \tag{40}$$

r is normalized to the beam rms size.

5.2 Percentage emittance

The reconstructed phase space distribution, with normalized coordinate against the rms beam size, can be directly used to calculate the percentage emittance, or the corresponding beam profile through Abel transform.

The fraction of beam inside a radius R in the (u, v) normalized phase space, is

$$\delta(R) = 2\pi \int_0^R \rho(r) r \, dr \tag{41}$$

Since R is normalized against rms beam size and beam rms emittance ϵ is calculated as described in section 4, the percentage emittance corresponding to δ is simply

$$\epsilon_\delta = R \, \epsilon \tag{42}$$

If it is ever needed, the fraction beam profile, that of the fraction in the central part of the phase space can be obtained by Abel transforming $\rho(r)$ with its value set to zero outside $r = R$.

As an example, a beam profile composed of a Gaussian plus a shoulder component is constructed and its corresponding phase space distribution is

calcuated using the technique described above. They are shown in Fig. 2. The fraction of beam calculation result compared with that of a Gaussian

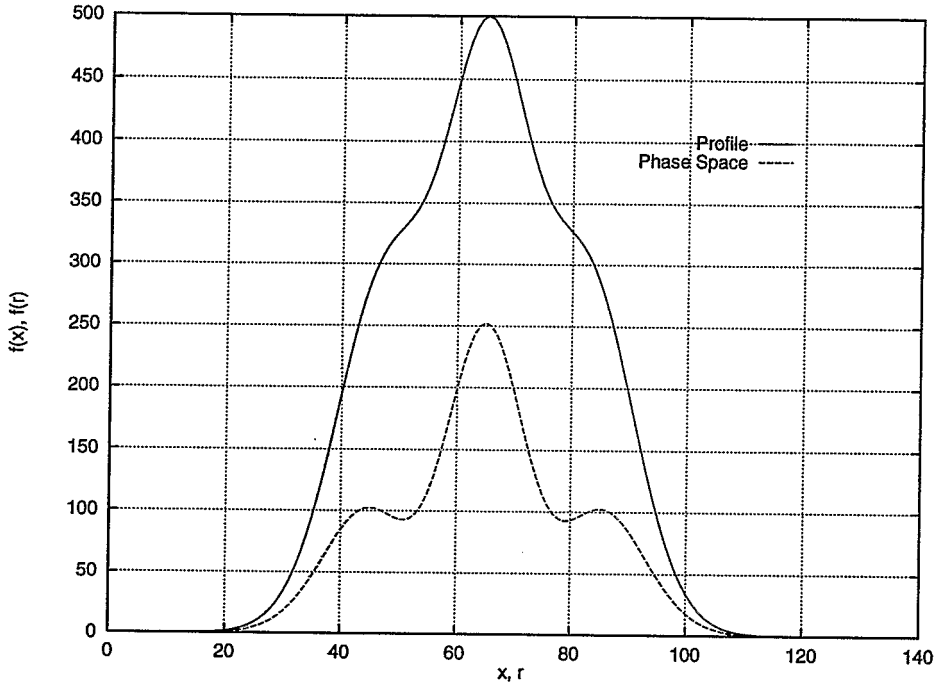

Figure 2: Beam profile and reconstructed phase space distribution.

beam is presented in Fig. 3.

5.3 Loss of elliptical symmetry and Radon inversion

In the case where elliptical symmetry assumed throughout this report, the reconstruction of phase space distribution theoretically need infinite number of profile measurements. Except the aspect ratio change that can happen in the beam phase space, the problem is the same as in computed tomography. To reconstruct a 2-dimensional object from all of its projections is the 2-dimensional Radon inversion problem. With the limited number of beam profiles we cannot expect to fully reconstruct, but nevertheless we should be able to extract some coarse features of the phase space distribution by using some of the numerical techniques in doing Radon inversion. This, however, will be left for future work.

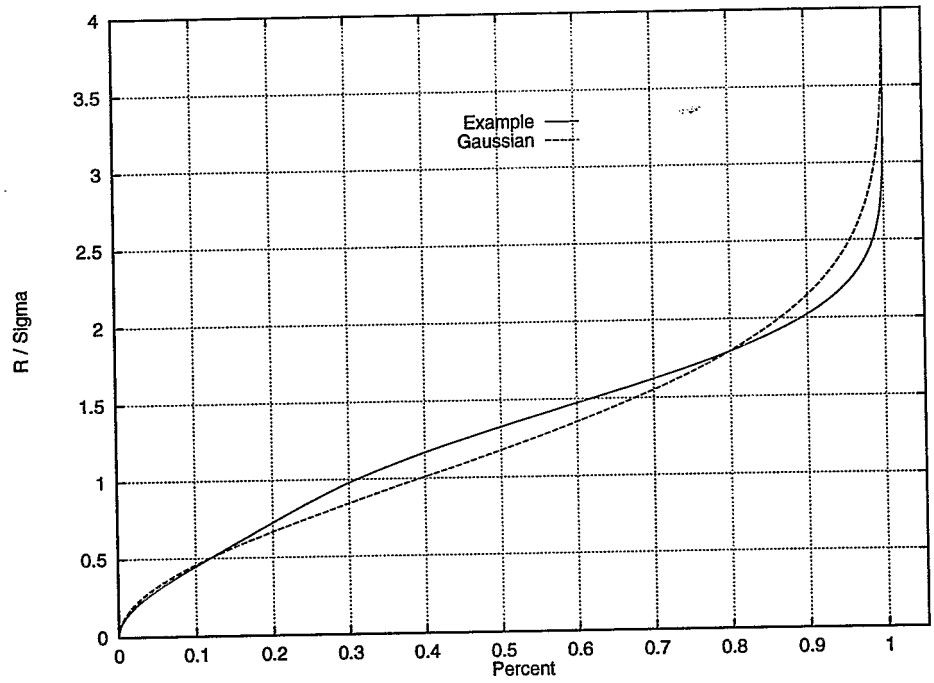

Figure 3: Fraction of beam plot compared with a Gaussian distribution..

A Abel inversion and fraction of beam calculation

Hermite polynomials and the related equations

$$H_n(x) = (-1)^n e^{x^2} \frac{d^n}{dx^n} e^{-\frac{x^2-r^2}{2}} = \sum_{k=0}^{[\frac{n}{2}]} \frac{(-1)^k n!}{k!(n-2k)!} (2x)^{n-2k} \tag{43}$$

$$H_{n+1}(x) = 2xH_n(x) - 2nH_{n-1}(x) \tag{44}$$

$$H_n'(x) = 2nH_{n-1}(x) \tag{45}$$

$$\int_{-\infty}^{\infty} H_m(x)H_n(x)\, e^{-x^2}\, dx = \begin{cases} 0, & m \neq n \\ 2^n n! \sqrt{\pi}, & m = n \end{cases} \tag{46}$$

Our profile function can thus be expanded into the Hermite polynomial

series:

$$f(x) = \sum_{n=0}^{\infty} h_n H_n(x) e^{-\frac{x^2-r^2}{2}} \tag{47}$$

with the coefficients being

$$h_n = \frac{1}{2^n n! \sqrt{\pi}} \int_{-\infty}^{\infty} f(x) H_n(x) e^{-\frac{x^2-r^2}{2}}\, dx \tag{48}$$

Since $H_n(-x) = (-1)^n H_n(x)$, for an even function $f(x)$ only even order Hermite polynomials will be involved.

The Abel inversion for each even order Hermite polynomials can be carried out recursively, as shown below.

$$\begin{aligned}
\widetilde{H}_{2m}(r) &\equiv -\frac{1}{\pi} \int_r^{\infty} \frac{\frac{d}{dx}[H_{2m}(x) e^{-\frac{x^2}{2}}]}{\sqrt{x^2-r^2}}\, dx \\
&= -\frac{1}{\pi} \int_r^{\infty} \frac{H'_{2m}(x) - x H_{2m}(x)}{\sqrt{x^2-r^2}} e^{-\frac{x^2}{2}}\, dx \\
&= \frac{1}{2\pi} \int_r^{\infty} \frac{H_{2m+1}(x) - 4m H_{2m-1}(x)}{\sqrt{x^2-r^2}} e^{-\frac{x^2}{2}}\, dx \\
&= [F_m(r) - 4m F_{m-1}(r)]\, e^{-\frac{r^2}{2}}
\end{aligned} \tag{49}$$

where

$$F_m(r) = \frac{1}{2\pi} \int_r^{\infty} \frac{H_{2m+1}(x)}{\sqrt{x^2-r^2}} e^{-\frac{x^2-r^2}{2}}\, dx \tag{50}$$

Using Eq. 44 and Eq. 45

$$\begin{aligned}
F_m(r) &= \frac{1}{\pi} \int_r^{\infty} \frac{x H_{2m}(x)}{\sqrt{x^2-r^2}} e^{-\frac{x^2-r^2}{2}}\, dx - 4m F_{m-1}(r) \\
&= \frac{1}{\pi} \int_r^{\infty} H_{2m}(x) e^{-\frac{x^2-r^2}{2}}\, d\sqrt{x^2-r^2} - 4m F_{m-1}(x) \\
&= -\frac{1}{\pi} \int_r^{\infty} \frac{H'_{2m}(x) - x H_{2m}(x)}{\sqrt{x^2-r^2}} (x^2-r^2) e^{-\frac{x^2-r^2}{2}}\, dx \\
&\quad -4m F_{m-1}(x)
\end{aligned} \tag{51}$$

Using Eq. 45 and Eq. 44 again gives us

$$\begin{aligned}
&F_m(r) + 4m F_{m-1}(r) \\
&= \frac{1}{2\pi} \int_r^{\infty} \frac{[H_{2m+1}(x) - 4m H_{2m-1}(x)]\,(x^2-r^2)}{\sqrt{x^2-r^2}} e^{-\frac{x^2-r^2}{2}}\, dx
\end{aligned} \tag{52}$$

With

$$\begin{aligned} x^2 H_{2m+1}(x) &= \frac{x}{2}\left[H_{2m+2}(x) + 2(2m+1)H_{2m}(x)\right] \\ &= \frac{1}{4}\left[H_{2m+3}(x) + 2(4m+3)H_{2m+1}(x)\right] \\ &\quad +2m(2m+1)H_{2m-1}(x) \end{aligned} \tag{53}$$

Eq. 52 yields the recursion relation for $F_m(r)$:

$$\begin{aligned} F_m(r) &= 2(2r^2 - 2m + 1)F_{m-1}(r) \\ &\quad -16(m-1)(r^2 - m + 1)F_{m-2}(r) \\ &\quad +8(2m-2)(2m-3)(2m-4)F_{m-3}(r) \end{aligned} \tag{54}$$

It will be easier to work with simple polynomials of r for the calculation of percentage emittance, so it is natual to rewrite Eq. 54 as

$$\begin{aligned} F_m(r) &= r^2\left[4F_{m-1}(r) - 16(m-1)F_{m-2}(r)\right] \\ &\quad -2(2m-1)F_{m-1}(r) + 16(m-1)^2 F_{m-2}(r) \\ &\quad +8(2m-2)(2m-3)(2m-4)F_{m-3}(r) \end{aligned} \tag{55}$$

Since in Eq. 45 and Eq. 44 the initial contributions from negative orders would not have appeared, Eq. 55 and Eq. 54 can be used with fewer terms at the beginning by simply droping the negatively ordered ones. The lowest ordered term can be calculated directly:

$$F_0(r) = \frac{1}{2\pi}\int_r^\infty \frac{H_1(x)e^{-\frac{x^2-r^2}{2}}}{\sqrt{x^2-r^2}}\,dx = \frac{1}{\sqrt{2\pi}} \tag{56}$$

With Eqs. 49,55 and 56, Abel inversion of all even order Hermite polynomials can be calculated easily numerically. We can also go a step furthur to formulate the calculation of the fraction of beam inside any phase space radius. This is can be done using Eq.55 and by expressing $F_m(r)$ as

$$F_m(r) = \sum_{l=0}^{m} g_l^m \cdot r^{2l} \tag{57}$$

Combining Eq. 55 and the following definition

$$g_l^m = 0, \quad l < 0,\ l > m \tag{58}$$

we obtain the recursion equation for g_l^m

$$\begin{aligned} g_l^m &= 4g_{l-1}^{m-1} - 16(m-1)\, g_{l-1}^{m-2} \\ &\quad -2(2m-1)\, g_l^{m-1} + 16(m-1)^2\, g_l^{m-2} \\ &\quad +32(m-1)(2m-3)(m-2)\, g_l^{m-3} \end{aligned} \tag{59}$$

The initial term is given by Eq. 56 and Eq. 57:

$$g_0^0 = \frac{1}{\sqrt{2\pi}} \tag{60}$$

The direct expansion from $\widetilde{H}_{2m}(r)$, the Abel inversion of $H_{2m}(r)$, to the powers of r is, from Eq. 49,

$$\widetilde{H}_{2m}(r) = F_m(r) - 4mF_{m-1}(r) = \sum_{l=0}^{m} G_l^m \cdot r^{2l} \tag{61}$$

where

$$G_l^m = g_l^m - 4m\, g_l^{m-1} \tag{62}$$

With

$$\int_0^\infty r^{2m} e^{-\frac{r^2}{2}}\, r dr = 2^m\, m! \tag{63}$$

the fraction of beam inside $r = R$ is

$$\begin{aligned} f(R) &= \frac{\sum_m h_m \int_0^R \widetilde{H}_{2m}(r)\, r dr}{\sum_m h_m \int_0^\infty \widetilde{H}_{2m}(r)\, r dr} \\ &= \frac{\sum_m \sum_l h_m G_l^m \int_0^R r^{2l} e^{-\frac{r^2}{2}}\, r dr}{\sum_m \sum_l h_m G_l^m \int_0^\infty r^{2l} e^{-\frac{r^2}{2}}\, r dr} \\ &= \frac{\sum_m \sum_l h_m G_l^m P_l(R)}{\sum_m \sum_l h_m G_l^m \cdot 2^l \cdot l!} \end{aligned} \tag{64}$$

where $P_l(R)$ follows yet another recursion relation:

$$P_m(R) = \int_0^R r^{2m}\, e^{-\frac{r^2}{2}}\, r dr = 2mP_{m-1}(R) - R^{2m} e^{-\frac{R^2}{2}} \tag{65}$$

$$P_0(R) = \int_0^R e^{-\frac{r^2}{2}}\, r dr = 1 - e^{-\frac{R^2}{2}} \tag{66}$$

References

[1] Richard L. Witkover. private communication, 1994.

[2] H. Ploss and L. N. Blumberg. Methods of emittance measurement in external beams using ellipse approximations. Internal Report AGS DIV 68-4, AGS/Brookhaven National Laboratory, November 1968.

[3] Kiyokazu Ebihara, *et al.* Non-destructive emittance measurement of a beam transport line. *Nuclear Instruments and Methods*, 202:403–409, 1982.

[4] Willianm H. Press, *et al.* *Numerical Recipes in C*, chapter 15. Cambridge University Press, 2nd edition, 1992.

[5] Karl L. Brown and Roger V. Servranckx. Optics modules for circular accelerator design. Technical Report SLAC-PUB-3957, SLAC, May 1986.

[6] Ronald N. Bracewell. *The Fourier Transform and Its Applications*, chapter 12. McGraw-Hill, 2nd edition, 1986.

[7] L. Montgomery Smith, Dennis R. Keefer, and S. I. Sudharsanan. Abel inversion using transform techniques. *Journal of Quantitative Spectroscopy and Radiative Transfer*, 39(5):367–373, 1988.